Nonlinear analysis of irregular animal vocalizations

Isao Tokuda[a)]
Department of Computer Science and Systems Engineering, Muroran Institute of Technology, Muroran, Hokkaido 050-8585, Japan

Tobias Riede and Jürgen Neubauer
Institute for Theoretical Biology, Humboldt-University of Berlin, Invalidenstrasse 43, D-10115 Berlin, Germany

Michael J. Owren
Department of Psychology, 224 Uris Hall, Cornell University, Ithaca, New York 14853

Hanspeter Herzel
Institute for Theoretical Biology, Humboldt-University of Berlin, Invalidenstrasse 43, D-10115 Berlin, Germany

(Received 20 October 2001; revised 6 March 2002; accepted 8 March 2002)

Animal vocalizations range from almost periodic vocal-fold vibration to completely atonal turbulent noise. Between these two extremes, a variety of nonlinear dynamics such as limit cycles, subharmonics, biphonation, and chaotic episodes have been recently observed. These observations imply possible functional roles of nonlinear dynamics in animal acoustic communication. Nonlinear dynamics may also provide insight into the degree to which detailed features of vocalizations are under close neural control, as opposed to more directly reflecting biomechanical properties of the vibrating vocal folds themselves. So far, nonlinear dynamical structures of animal voices have been mainly studied with spectrograms. In this study, the deterministic versus stochastic (DVS) prediction technique was used to quantify the amount of nonlinearity in three animal vocalizations: macaque screams, piglet screams, and dog barks. Results showed that in vocalizations with pronounced harmonic components (adult macaque screams, certain piglet screams, and dog barks), deterministic nonlinear prediction was clearly more powerful than stochastic linear prediction. The difference, termed low-dimensional nonlinearity measure (LNM), indicates the presence of a low-dimensional attractor. In highly irregular signals such as juvenile macaque screams, piglet screams, and some dog barks, the detectable amount of nonlinearity was comparatively small. Analyzing 120 samples of dog barks, it was further shown that the harmonic-to-noise ratio (HNR) was positively correlated with LNM. It is concluded that nonlinear analysis is primarily useful in animal vocalizations with strong harmonic components (including subharmonics and biphonation) or low-dimensional chaos. [DOI: 10.1121/1.1474440]

PACS numbers: 43.80.Ka, 43.80.Lb, 43.25.Rq [WA]

I. INTRODUCTION

Animal vocalizations range from almost harmonic to completely noisy sounds (Tembrock, 1996; Hauser, 1996; Bradbury and Vehrencamp, 1998),[1] where calls containing noisy elements in various amounts are referred to as ''atonal'' (Tembrock, 1976; Hauser, 1993). Such sounds are characterized by broadband spectra with energy at many different frequencies and sometimes with traces of harmonic elements. A prototype of such vocal utterances is the ''scream,'' which is a vocalization described in the acoustic repertoires of many species (for instance, humans: Michelsson, 1980; macaques: Rowell, 1967; Grimm, 1967; Green, 1975; Hohmann, 1989; Gouzoules and Gouzoules, 2000; pigs: Schön *et al.*, 1999). Another typical atonal utterance is the ''bark'' which is present in the repertoire of several species, including primates (macaques: Struhsaker, 1967; Green, 1975; baboons: Hall and DeVore, 1965) as well as canids (Tembrock, 1976; Schassburger, 1993; Feddersen-Petersen, 2000). In those categories, various types of calls are often considered to be the same regardless of the difference in their functions or significances. For instance, in canids different functions have been ascribed to barks depending on the ratio of harmonic to nonharmonic energy in these vocalizations (Tembrock, 1976; Wilden, 1997; Feddersen-Petersen, 2000). Until now those differences have been rarely considered because of the difficulty of quantifying small variation between calls which are spectrally very similar (Owren and Linker, 1995). While statistical approaches like the multiparametric analysis (Schrader and Hammerschmidt, 1997) have been able to uncover statistical differences by using many acoustic parameters (Fischer *et al.*, 1995), the relationship between these parameters and the sound production mechanisms involved is not clear.

Understanding sound production mechanisms might help explain the communicative role of such atonal animal vocalizations by allowing spectral variability to be differentially ascribed to anatomical and motivational factors. Atonal

a)Author to whom correspondence should be addressed: electronic mail: tokuda@csse.muroran-it.ac.jp

 0001-4966/2002/111(6)/2908/12/$19.00

sounds are in general due to complex vocal production mechanisms such as regular and irregular vocal-fold vibrations as well as turbulent noise generated in the vocal tract (Davis and Fletcher, 1996). Vocal-fold vibration has been extensively studied in humans (reviewed in Titze, 1994), whereas few studies exist in nonhuman mammals (Paulsen, 1967; Brown and Cannito, 1995; Brown *et al.,* 2002).

The concept of ''nonlinear dynamics'' has been recently introduced to animal bioacoustics, where characteristics of vocalizations are classified using the terminology of dynamical systems (Wilden *et al.,* 1998). (i) Limit cycle: the spectrum is composed of a fundamental frequency with harmonics that are integer multiplies of that frequency. (ii) Subharmonics: additional spectral components appear in the harmonic stack, typically at multiples of 1/2 or 1/3 of the fundamental frequency. (iii) Biphonation: the simultaneous occurrence of two independent fundamental frequencies. (iv) Chaos: a broadband segment with no particular harmonics in the spectrum. (v) Bifurcations: transitions between different nonlinear dynamical states. Acoustic analyses of birds (Fee *et al.,* 1998) and mammals (Wilden *et al.,* 1998; Fitch *et al.,* 2002) have shown a variety of such nonlinear phenomena, including rapid transitions from harmonic to subharmonic and chaotic states without intervening silent intervals. These observations suggest that the transitions arise from intrinsic properties of the vibrating components of the larynx. The intrinsic dynamics of the vocal folds can thus produce complex temporal acoustic call patterns without complex nervous system control (Fitch *et al.,* 2002).

The theory of nonlinear dynamics shows that rather complex vocalizations can be generated from systems described by nonlinear equations of motion having very few dynamical variables. For example, the desynchronization of horizontal and vertical vibratory modes of the vocal folds (Berry *et al.,* 1994) or the desynchronization of the left and the right vocal folds (Steinecke and Herzel, 1995; Tigges *et al.,* 1997) can lead to subharmonics, biphonation, and low-dimensional deterministic chaos. Such observations imply that some of the noisy animal utterances which have been considered as turbulent noise or high-dimensional dynamics might be generated from low-dimensional nonlinear systems. In order to quantify the complexity of animal vocalizations, it therefore becomes quite important to clarify whether the underlying dynamics are low-dimensional or high-dimensional.

Dynamical systems are considered low-dimensional if they exhibit only a few (say, 3 to 10) dynamical components and high-dimensional if they have many more. Typical examples of low-dimensional dynamics in acoustics are certain pathological voices (Titze *et al.,* 1993) and musical instruments under certain conditions (Gibiat and Castellengo, 2000). An example of high-dimensional dynamics, on the other hand, is turbulent air flow. However, since broadband spectra do not always imply low-dimensional dynamics, special analysis techniques based on nonlinear dynamics should be applied to distinguish low-dimensional systems from high-dimensional ones.

From the point of view of animal voice production, detection of low-dimensionality in acoustic signals is of particular interest. In principle, acoustic signals are the result of the neural control of the vocal production system (respiratory system, larynx, and vocal tract), which has rich biomechanical properties. Nonetheless, it has been found in nonlinear studies of voice that even without complex nervous system control the vocal system can exhibit a variety of complex nonlinear phenomena such as chaos and bifurcations (Mende *et al.,* 1990; Titze *et al.,* 1993). Observations of low-dimensional dynamics therefore imply that a variety of complex features of animal vocalizations is traceable primarily to the biomechanical properties of the vocal production systems involved rather than close neural control *per se*.

Nonlinear analysis of animal vocalizations may have significant importance for animal communication research. For instance, in animal bioacoustics, sounds are often categorized as being either harmonic or atonal. Calls with mixed structural components (e.g., harmonic calls with noisy overlay or calls in which tonal and noisy components are interspersed) have been excluded from most analyses (e.g., Hauser, 1993) or considered as atonal. This poor dichotomy makes systematic studies of animal acoustic communication difficult (Ryan, 1988; Hauser, 1993). The harmonic-to-noise ratio has been recently introduced in order to improve differentiation among atonal calls (Riede *et al.,* 2001). The question of whether atonal calls are low dimensional or high dimensional, however, remains unresolved. This issue is important because we can differentiate three main sources of voice irregularities: (a) air turbulence generated in the vocal tract, (b) high-dimensional complex vocal-fold vibration, and (c) low-dimensional irregular vocal-fold vibration. Precise quantification of the degree of irregularity is therefore important for studies of animal communication.

For human speech signals, nonlinear analysis has been carried out rather extensively (Mende *et al.,* 1990; Townshend, 1991; Titze *et al.,* 1993; Herzel *et al.,* 1994; Narayanan and Alwan, 1995; Kubin, 1995; Kumar and Mullick, 1996; Behrman *et al.,* 1998; Behrman, 1999). For animal voice signals, however, nonlinear characteristics have not yet been thoroughly investigated. Narrow-band spectrographic analysis has been proven to be useful in interpreting nonlinear phenomena such as limit cycles, subharmonics, biphonation, chaotic episodes, and transitions among different nonlinear dynamical states (Wilden *et al.,* 1998; Fitch *et al.,* 2002). Simply counting the various phenomena has provided the first quantitative results (Riede *et al.,* 1997, 2000), but further application of more sophisticated techniques like Lyapunov exponents and fractal dimensions (Titze *et al.,* 1993; Fletcher, 2000) can be problematic as these measures are quite sensitive to nonstationarities that are common in animal signals.

In this paper, a new method is introduced to analyze nonlinear dynamics of animal voices. Some decades ago, any irregularity in signals was attributed to random noise and consequently, broadband signals have been modeled typically with linear stochastic models such as autoregressive (AR) models. With the advent of chaos theory (May, 1976), it became clear that irregularities may be due to deterministic chaos in low-dimensional nonlinear systems. In order to distinguish two sources of irregularities, Farmer and Sidorow-

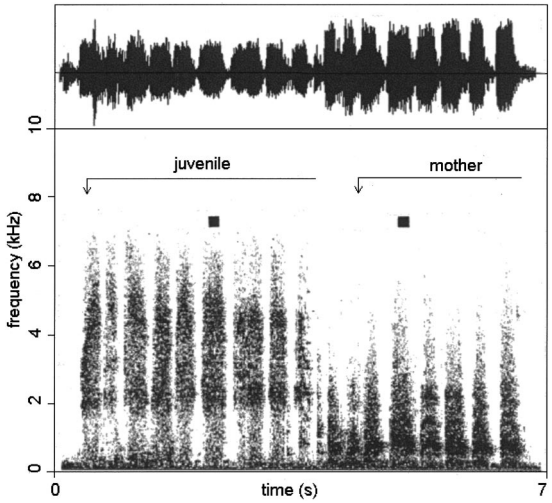

FIG. 1. Time series of the macaque screams (above) and its spectrogram (below). The first nine calls (marked with arrow as ''juvenile'') were from 1-year old juvenile, the tenth call was ambiguous, and the remaining calls (marked with arrow as ''mother'') were from the mother. The black markers above the spectrogram indicate the segments used for the DVS analysis. The juvenile's calls started when it became frightened due to the proximity of an alpha male. Then the mother came running over and began screaming, which drew the male's attention to her.

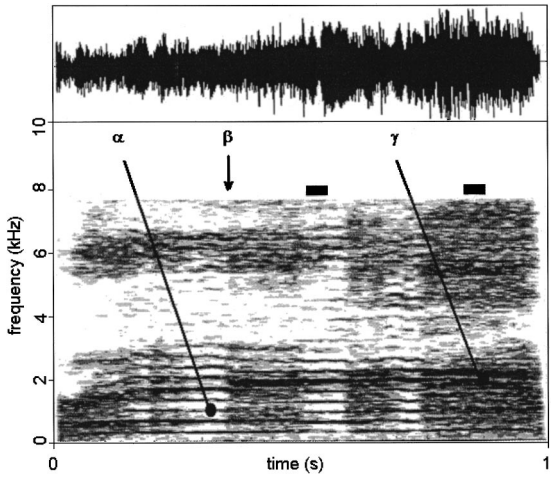

FIG. 2. Time series of a piglet scream (above) and its spectrogram (below). The black markers indicate the regions associated with harmonic and noisy spectral structures, which were analyzed using the DVS technique in Fig. 8. The arrows are directed to limit cycle with harmonic regime (α), bifurcation with a sudden transition between two different regimes (β), and complex dynamics with broadband spectral regime (γ).

ich (1987) suggested evaluating the predictive power of deterministic nonlinear models and stochastic linear models. By comparing the deterministic nonlinear predictability with the stochastic linear predictability, the strength of nonlinearity in the data can be measured. After this concept, the method is called the ''deterministic nonlinear versus stochastic linear (DVS)'' modeling technique (Farmer and Sidorowich, 1987; Casdagli, 1992). Here, we apply the DVS modeling technique to macaque screams, piglet screams, and dog barks as three examples of complex animal vocalizations. On the basis of further analysis of 120 samples of dog barks, we also examined the correlation between degree of nonlinearity and harmonic-to-noise ratios in the same signals.

II. MATERIAL

Voice data from Japanese macaques (*Macaca fuscata*), piglets (*Sus scrofa forma domestica*), and domestic dogs (*Canis lupus forma domestica*) were analyzed as representatives of atonal animal vocalizations.

The macaque screams were recorded from a 1-year-old juvenile and its adult-female mother, and digitized with a sampling frequency of 22 kHz. Figure 1 shows the time series of these screams, as well as a spectrogram computed with a 512-point FFT. The first nine calls are from the juvenile, the tenth sound is ambiguous, and the remaining screams are all from the mother. The broadband spectra apparent in the spectrogram show that neither the juvenile's scream nor the mother's call have a simple harmonic structure associated with fundamental frequencies.

As a next example, screams were recorded from six piglets (age: 16 days, body mass: 4.1 ± 0.9 kg) with a sampling frequency of 20 kHz. Figure 2 shows an example of the piglet scream and its corresponding spectrogram. The spectrogram shows that transitions among harmonic sounds with several peak frequencies and irregular sounds with broadband spectra occur in the series of the piglet scream.

As a final example, barks were recorded from 6 dogs (named as a, b, c, d, e, and f) with a sampling rate of 20 kHz. All dogs were from the breed dachshund, ranged in weight between 7.9 and 10.7 kg. The dogs a, b, e, and f belong to a clinic sample, where the barks were recorded while treated in a veterinary clinic for some disorders. The dogs c and d, on the other hand, are normal and healthy dachshunds whose barks were recorded at the owner's property. The barks were elicited by staring into dog's eyes (a mild threat to the animal), where only the dogs from which the barkings could be elicited in this way were used for the analysis. Samples of the dog barks used in the present study come from the samples used by Riede *et al.* (2001). Selection criterion was the dog's harmonic-to-noise-ratio (HNR) value averaged over its first 50 calls per recording session. The HNR is a measure that compares the acoustic energy of the harmonic components with that of the noise in time series. This measurement has been introduced to study hoarseness of human voice (Yumoto *et al.*, 1982; Awan and Frenkel, 1994). A voice with low HNR sounds quite hoarse, whereas a voice with high HNR is tense or pressed. According to the HNR analysis applied to 20 samples of dogs, the dogs a and b had the lowest average HNR (1st and 2nd rank), the dogs c and d had a medium HNR (14th and 16th rank), and the dogs e and f had the highest average HNR (19th and 20th rank). In the present study, 20 barks recorded from each dog were analyzed. Figure 3 shows three different dog barks and their corresponding spectrograms (bark A from dog a: HNR=9; bark B from dog c: HNR=13; bark C from dog f: HNR=17). The spectrograms show that several sharp peaks are observed in the frequency structure of the bark C, whereas the sharp frequency structure is flattened in the bark B, and is quite broad in bark A.

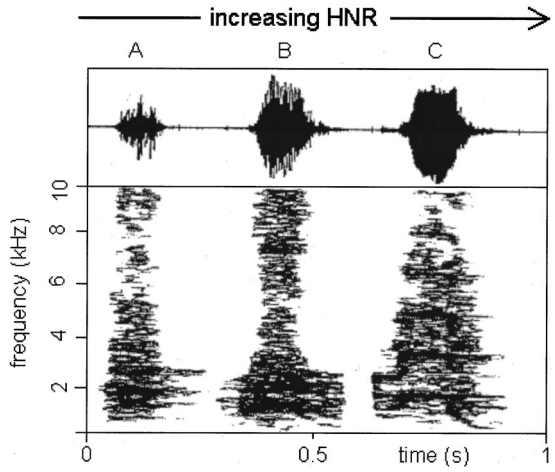

FIG. 3. Time series (above) of three dog barks with low (A); medium (B); and high (C) HNR and their corresponding spectrograms (below). The barks A, B, and C were recorded from the dogs a, c, and f, respectively.

III. METHODS

In the field of nonlinear dynamics, various techniques have been developed to estimate nonlinear dynamical quantities such as fractal dimensions and Lyapunov exponents from time series (for instance see reviews by Lauterborn and Parlitz, 1988; Abarbanel, 1996; Kantz and Schreiber, 1997). One must be careful in using such techniques, because reliable estimation of these quantities from short-term data requires delicate numerical computation (Theiler, 1986; Smith, 1988; Ruelle, 1990). The analysis of long-term voice data, on the other hand, suffers from nonstationarity. In addition, the contamination of the data with noise often gives rise to spurious results for dimension estimates (Ruelle, 1994; Rapp, 1993; Rapp *et al.*, 1993).

The DVS modeling technique introduced by Casdagli (1992) provides a more robust approach. In general, there are two major approaches to model irregular time series in nature: (A) deterministic nonlinear prediction model (Farmer and Sidorowich, 1987) and (B) stochastic linear prediction model (Markel and Gray, 1976). The main idea of DVS technique is to measure the strength of nonlinearity by comparing the prediction accuracy of the two models. If the data represent at least partially a low-dimensional attractor, its nonlinear dynamical components can be predicted by using nonlinear models. Linear prediction models, on the other hand, cannot accurately predict nonlinear dynamical components. The strength of the nonlinearity in the time series can therefore be measured as the gap between the nonlinear prediction error and the linear prediction error. The method is quite simple and effective for short-term noisy data, with applications to many real-world data such as coupled diodes, fluid turbulence, flame dynamics, human speech, EEG data, measles, and sunspots (Casdagli, 1992).

DVS analysis of the animal voice data was conducted as follows. First, we embedded the time series $\{x_t : t = 1,2,...,N\}$ into delay coordinate space (Takens, 1981; Sauer *et al.*, 1991)

$$\mathbf{x}(t) = (x_t, x_{t-\tau}, x_{t-2\tau}, \ldots, x_{t-(d-1)\tau}) \tag{1}$$

(d: embedding dimension, τ: delay time). In this particular analysis, the delay time was always set to be $\tau = 1$. By setting the embedding dimension d large enough, we get information of the basic waveform structure (in the case of periodic data, this corresponds to one period of the waveform) within the time length $d-1$ of the vector $\mathbf{x}(t)$. For a data point $\mathbf{x}(t)$, distances from other points $\mathbf{x}(s)$ were computed as $d_{t,s} = \|\mathbf{x}(t) - \mathbf{x}(s)\| = \sqrt{\Sigma_{i=0}^{d-1} (x_{t-i} - x_{s-i})^2}$ $(s = d, d+1, ..., N)$. By ordering the distances as $d_{t,s(1)} \leqslant d_{t,s(2)} \leqslant \cdots \leqslant d_{t,s(N-d+1)}$, D neighbors $\{\mathbf{x}(s(i)) : i = 1,2,...,D\}$ of $\mathbf{x}(t)$ were found. Note that the data point itself and its temporally close points $\{\mathbf{x}(s) : |s-t| \leqslant 15\}$ were not included in the neighbors (Theiler, 1986). Then, one step further state of x_t was predicted by using a local linear predictor as

$$\tilde{x}_{t+1} = \sum_{k=0}^{d-1} a_k(t) x_{t-k}, \tag{2}$$

where the prediction coefficients $\{a_0(t), a_1(t), \ldots, a_{d-1}(t)\}$ were determined by a least-square algorithm, minimizing the error function defined for the D neighbors as

$$E(a(t)) = \sum_{i=1}^{D} \left\{ x_{s(i)+1} - \sum_{k=0}^{d-1} a_k(t) x_{s(i)-k} \right\}^2. \tag{3}$$

This technique is called local linear prediction because the ''local'' dynamics of the data is approximated by ''linear'' models. Note that the ''local linear'' implies essentially a nonlinear model since the prediction model depends on the location of the data $\mathbf{x}(t)$ in coordinate space. Consequently, local linear models are also capable of generating deterministic chaos. The difference of the predicted signal $\tilde{x}_t$ and the true signal x_t measures the prediction accuracy. Using the residual signals: $r_t = x_t - \tilde{x}_t$, the signal-to-noise ratio (SNR) was computed as

$$\mathrm{SNR} = 10 \log \left(\frac{\Sigma_{t=d}^{N} \{x_t - \overline{x}\}^2}{\Sigma_{t=d}^{N} \{r_t - \overline{r}\}^2} \right) \mathrm{dB}, \tag{4}$$

where

$$\overline{x} = \frac{1}{N-d+1} \sum_{t=d}^{N} x_t, \quad \overline{r} = \frac{1}{N-d+1} \sum_{t=d}^{N} r_t.$$

Here, noise refers to unpredictable components within the signal.

This local linear prediction shows a remarkable dependence on the number of the neighbors [see Fig. 4, where $\#N = 100 \cdot D/(N-d+1)\%$ stands for a percentage of the number of the neighbors among all data points $\{\mathbf{x}(s) : s = d, d+1, ..., N\}$]. In the case of a small number of neighbors, prediction accuracy is sensitive to recording noise (meaning energy from a different source than the animal's vocal apparatus) contained in the data. This sensitivity results in a relatively low SNR. As the number of the neighbors is increased, the recording noise effect is suppressed, nonlinear structure of the data is well modeled by local linear predictor, and consequently the SNR is improved. With an intermediate number of the neighbors, the highest SNR with optimum nonlinear prediction is realized. As the number of the neighbors is further increased ($\#N \to 100\%$), the local linear pre-

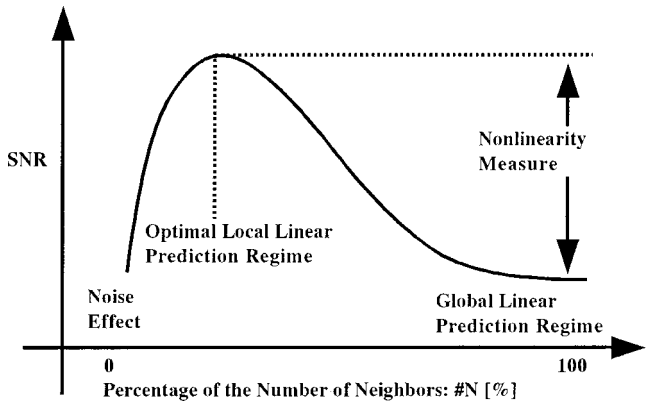

FIG. 4. Schematic illustration of the DVS plot. In the case of small #N, the SNR is low due to noise contained in the data. As #N is increased, the SNR is improved and optimized at an intermediate value of #N. As #N is further increased, the SNR is again lowered. The low-dimensional nonlinearity measure (LNM) is defined as an SNR gap between the optimal nonlinear prediction regime and the global linear prediction regime.

dictor eventually becomes close to a global linear predictor. This global linear model is almost identical to an AR model, except that in the parameter estimation it does not use temporally correlated data (AR modeling uses the complete data set). Nonlinear components cannot be well predicted by the global linear model and the SNR is again lowered. Depending on the strength of nonlinearity of the data, a gap should be observed between optimal nonlinear prediction and global linear prediction. If the nonlinearity of the data is strong (or weak), the gap should be large (or small). By using this property, the amount of nonlinearity included in the data can be measured.

Finally, we define the low-dimensional nonlinearity measure (LNM) as an SNR gap between the optimal nonlinear prediction and the linear prediction as

$$\mathrm{LNM} = \mathrm{SNR}_{\text{optimal nonlinear prediction}} - \mathrm{SNR}_{\text{global linear prediction}} \mathrm{dB}. \quad (5)$$

LNM can be interpreted as the amount of the signal that cannot be predicted by the linear model but is predicted by the nonlinear model. We note that in case of analyzing complex data generated from high-dimensional nonlinear systems, it is not easy for any modern technique (Lauterborn and Parlitz, 1988; Abarbanel, 1996; Kantz and Schreiber, 1997) to precisely detect nonlinearity in the data, because such data often cannot be distinguished from the ones generated from complex stochastic dynamics. We therefore emphasize that the LNM is to detect *low-dimensional* nonlinearity in data.

IV. ANALYSIS OF A PATHOLOGICAL VOICE

As a benchmark test for the DVS technique described in Sec. III, a pathological voice was first analyzed. Since nonlinear dynamics of pathological voices has been well analyzed (Titze *et al.*, 1993), such a voice sample provides good data for testing the DVS technique. Figure 5(a) shows the time series of a pathological voice recorded at the university hospital (Charité) of the Humboldt-University of Berlin from a female subject who had papillomas of the vocal folds. The

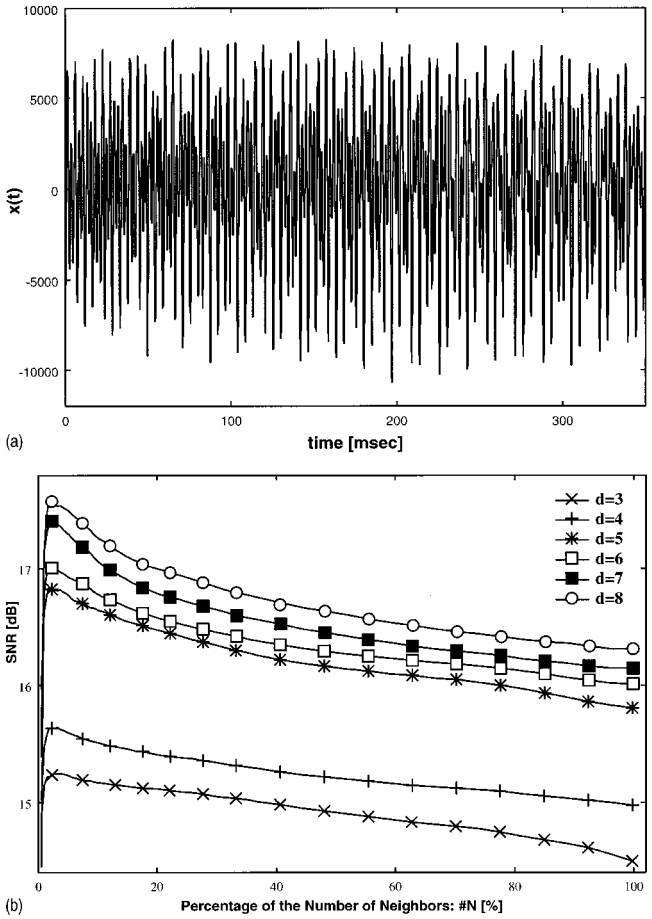

FIG. 5. (a) Waveform structure of the pathological voice. (b) DVS plot of the pathological voice.

data were digitized with a sampling frequency of 20 kHz and 12-bit resolution. By removing the initial transient phase and the final decay phase, the stationary part of the vowel /u/ composed of $N=7000$ data points was extracted. Nonlinear property of this voice sample was carefully investigated by Titze *et al.* (1993). By delay coordinate embedding technique, low-dimensional strange geometrical structure of the pathological voice was reconstructed. By fractal dimensional analysis, a noninteger dimension of $D_2=2.6$ was estimated. By Lyapunov spectrum analysis, positive first Lyapunov exponent of $\lambda_1 \approx 0.1\ \mathrm{ms}^{-1}$ indicating orbital instability of the data was estimated. These analysis results provided strong evidence for low-dimensional chaos in the pathological voice sample.

Figure 5(b) shows the result of the DVS analysis applied to the pathological voice data. The DVS plots were drawn for varying the embedding dimension $d=3,4,...,8$. For all DVS plots with different embedding dimensions, clear peak structures of the SNR at an intermediate number of neighbors were discernible. Namely, as the percentage of the number of the neighbors #N was increased from zero, the SNR increased with a peak at about #$N=3\%$. As the number of neighbors was further increased from the peak, then the SNR decreased monotonically. This result implies that the pathological voice contains a certain amount of low-dimensional nonlinearity that gives rise to a clear gap between nonlinear prediction error and linear prediction error. For a variety of

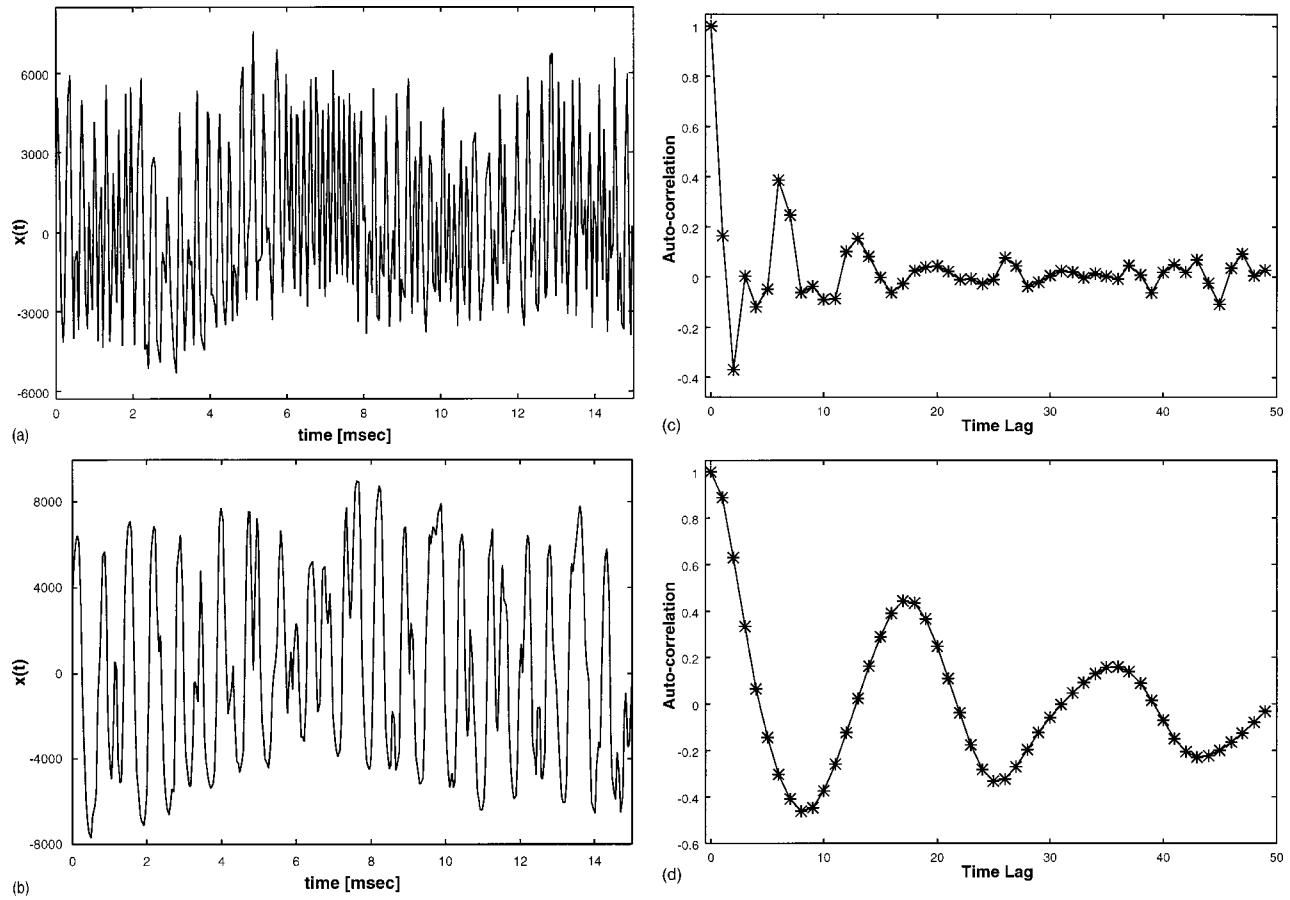

FIG. 6. (a) Enlarged waveform structure of the juvenile macaque's scream of Fig. 1. (b) Enlarged waveform structure of the mother macaque's call of Fig. 1. (c) Autocorrelation function of the juvenile macaque's scream. (b) Autocorrelation function of the mother macaque's call.

embedding dimensions, a nonlinearity measure LNM was in the order of 1 dB. Since this voice sample was shown to have low-dimensional chaotic property, we may say that the present DVS technique works for real acoustic data and the nonlinearity measure LNM of 0.5 dB implies existence of low-dimensional nonlinear dynamics in the data.

V. RESULTS

A. Macaque screams

Analyzing macaque screams as a first example of animal vocalization, Figs. 6(c) and (d) show autocorrelation functions for the calls from the juvenile and its mother, respectively. While the autocorrelation function for the juvenile's scream showed rapid decay, the mother's call gave rise to a function with a long tail. Strong correlation implies periodic structure, whereas weak correlation implies noisy structure. The long-term correlation of the mother's call reflected the waveform structure of Fig. 6(a), which showed relatively clear periodicity. The vanishing correlation of the juvenile's scream, on the other hand, might be due to the noisy waveform structure of Fig. 6(b). Figures 7(a) and (b) show results of the DVS analysis applied to screams of the juvenile and the mother. The DVS plots were drawn for varying embedding dimension $d=3,4,...,8$. In both figures, clear peak structures of the SNR at an intermediate number of neighbors were apparent. The peaks were observed at $\#N=3.33\%$ for the juvenile and $\#N=2.5\%$ for the mother. As the number of neighbors was increased from the peak point, SNR decreased monotonically. This result implies that both calls contain a certain amount of nonlinearity that gave rise to a gap between nonlinear prediction error and linear prediction error. Compared to the juvenile's scream, the mother's call showed a larger gap. In fact, in the case of $d=7$, the nonlinearity measure was LNM$=0.23$ dB for the juvenile and LNM $=0.50$ dB for the mother. As we have seen from the analysis of the pathological voice, LNM of more than 0.5 dB can point to low-dimensionality in acoustic signal. We may therefore say that the mother's call had low-dimensional nonlinear characteristic, whereas nonlinearity of the juvenile's scream was not so clear. This outcome might be due to the periodic components of the mother's call, as limit-cycle dynamics, which were well predicted by nonlinear models. The irregular dynamics of the juvenile macaque's calls seemed to reflect high-dimensional dynamics, since the nonlinear model with embedding dimension up to 8 allowed only a small improvement of the linear prediction.

B. Piglet screams

As a second example of an animal voice, piglet screams were analyzed. Figures 8(a) and (b) show results of the DVS analysis applied to the piglet scream of Fig. 2, where (a) corresponds to the harmonic sound region of Fig. 2 and (b) corresponds to the noisy scream region. The DVS plots were drawn by varying the embedding dimension as $d=3,...,8$.

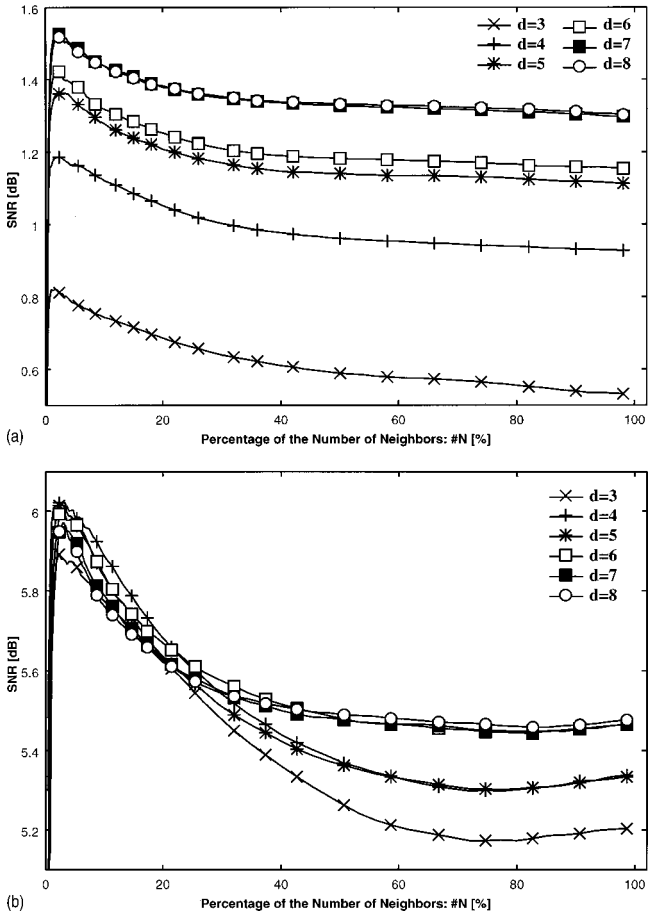

FIG. 7. (a) DVS plot of the juvenile macaque's scream of Fig. 6(a). (b) DVS plot of the mother macaque's scream of Fig. 6(b).

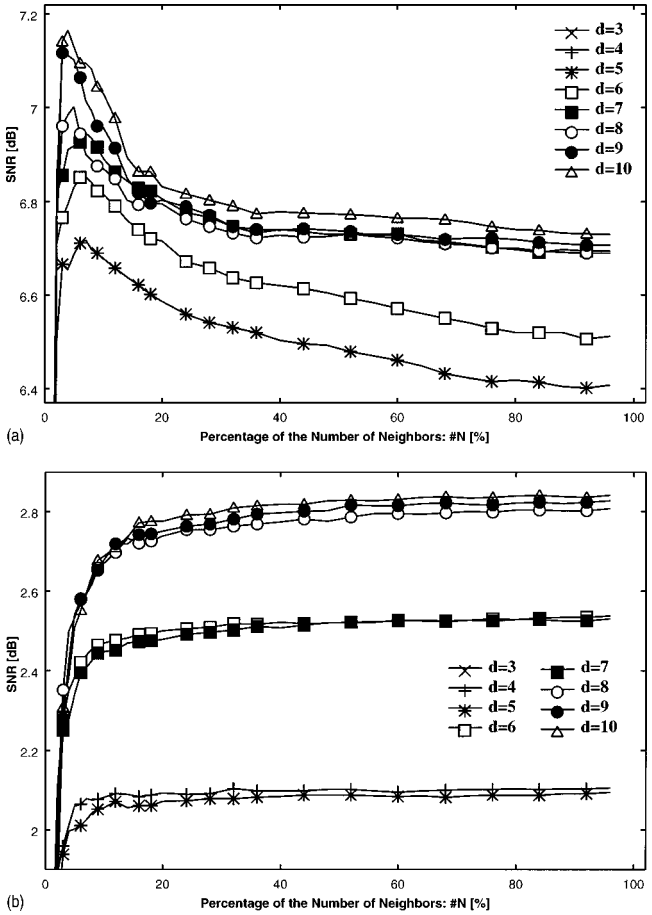

FIG. 8. (a) DVS analysis of the piglet scream extracted from the first marker in Fig. 2. (b) DVS analysis of the piglet scream extracted from the second marker in Fig. 2.

The harmonic part showed a large nonlinearity measure LNM, meaning a large gap between nonlinear prediction and linear prediction. The noisy part, on the other hand, did not exhibit such behavior. More specifically, in the case of $d=9$, the nonlinearity measure was LNM$=0.41$ dB for the harmonic part and LNM$=0$ dB for the noisy part. Conducting the same analyses with various screams from 5 other piglets produced similar results. Namely, strong nonlinearity was detected in harmonic screams, whereas no clear evidence for nonlinear dynamics was found in noisy screams. Hence, the harmonic parts of piglet screams can be considered to be due to low-dimensional nonlinear dynamics such as limit cycle, subharmonics, and biphonation (see the region indicated as α in Fig. 2 as an example of limit cycle regime). In contrast, the noisy parts may be due to turbulent noise or high-dimensional complex dynamics.

C. Dog barks

As the final example, we analyzed dog barks. First, three dog barks with low, medium, and high HNR (barks A, B, and C shown in Fig. 3) were tested. Figures 9(a), (b), and (c) show results of the DVS analysis applied to the three dog barks. As the HNR level increases from low to high (from bark A to B to C), the DVS plot gives rise to clearer peaks at an intermediate number of neighbors and the gap between nonlinear prediction regime and linear prediction regime becomes larger. In the case of $d=8$, the nonlinearity measure was LNM$=0.02$ dB for bark A with low HNR, LNM $=0.18$ dB for bark B with medium HNR, and LNM $=1.23$ dB for bark C with high HNR. These results imply that barks with high HNR exhibit low-dimensional dynamics. The irregular components included in the hoarse barking with low HNR may have been from turbulent noise or high-dimensional dynamics.

A further, more comprehensive analysis examined 120 barks recorded from the 6 dogs a, b, c, d, e, and f (20 barks from each). As shown in Fig. 10, the dog barks exhibit various waveform patterns [(a) and (b): two different barks of dog a, (c) and (d): two different barks of dog f]. Even in a single dog, the repeated barks exhibited different waveform structures. The relationship between the HNR and the nonlinearity measure LNM of the 120 barks is shown in Fig. 11(a), based on the computation of the LNM with fixed parameters of $d=5$ and $\#N=4.8\%$ for the nonlinear prediction. HNR and LNM were found to be correlated, with a correlation coefficient of $r=0.647$. In order to unfold the correlation curve, a ranked correlation plot is presented in Fig. 11(b), where the HNR (or the LNM) values are normalized between 0 and 1 in such a way that the ith-ranked HNR (or LNM) is given a value of $i/120$. A qualitatively similar structure to Fig. 11(a) is discernible with a ranked correlation coefficient of $r=0.646$. Hence, we may conclude that the

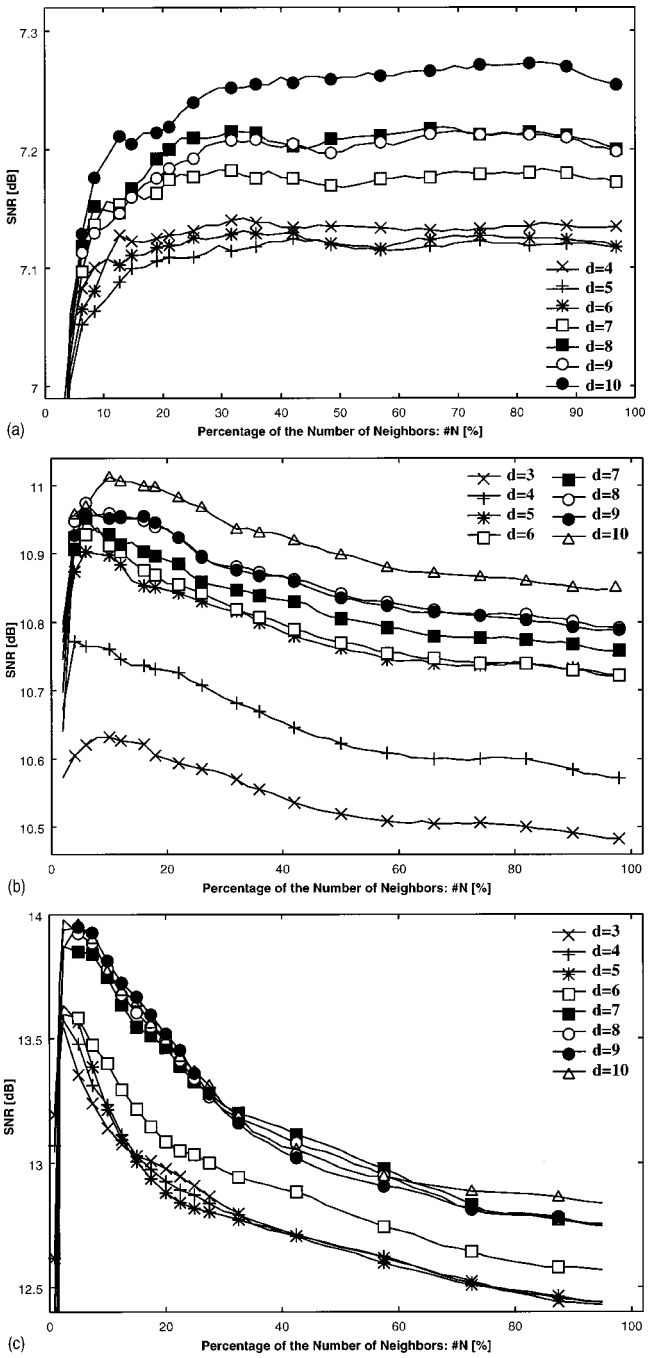

FIG. 9. (a) DVS plots of the dog bark with low HNR value (bark A of Fig. 3). (b) DVS plots of the dog bark with medium HNR value (bark B of Fig. 3). (c) DVS plots of the dog barks with high HNR value (bark C of Fig. 3).

nonlinearity measure LNM increased with the HNR. This result implies that nonlinearities are observed in dog barks mainly when they have clear harmonic dynamical components, such as limit cycles, subharmonics, and biphonation.

It should be noted that the correlation plots of Fig. 11 include several outliers which exhibit relatively strong nonlinearity measure LNM at intermediate HNR levels. There is a possibility that such relatively noisy barks are generated from low-dimensional nonlinear dynamics such as chaos. Careful investigation of these presumably chaotic data is thus an interesting research subject for future studies.

VI. SURROGATE ANALYSIS

In this section, we test the significance of nonlinearity observed in the animal vocalizations in Sec. V. In nonlinear data analysis, it is quite important to clarify the underlying dynamical process that has been detected by the nonlinear method. This clarification, however, is quite difficult, since there are a variety of stochastic processes that look similar to nonlinear dynamics. As a first approach to validate nonlinear analysis of irregular animal vocalizations, we carried out a surrogate analysis (Theiler *et al.*, 1992). The surrogate analysis is a kind of statistical hypothesis testing, which is to test a null hypothesis that the acoustic signal is generated from a particular class of stochastic dynamical process. In accordance with the null hypothesis, sets of artificial time series, called *surrogate data*, which preserve some of the statistical properties of the original signal are created. Then, a discriminating statistic is computed for the original and the surrogate data. If the discriminating statistic of the original signal is significantly different from those of the surrogate data, the null hypothesis can be rejected. The surrogate data have the property of ''constrained-realization'' (Theiler and Prichard, 1996), which is to randomize the original data by strictly preserving some of the original statistical quantities. It has been empirically known that the surrogate analysis is effective for statistical hypothesis testing when nonlinear dynamical quantity is utilized as a discriminating statistic.

In this study, as a standard surrogate analysis, we tested a null hypothesis that the macaque screams were generated from linear Gaussian dynamical process. Here, an iterative Fourier transformed algorithm (Schreiber and Schmitz, 1996) was utilized to shuffle the original signal and to generate surrogate data, which exactly preserved the original histogram and approximately preserved the original power spectrum. The local linear prediction error was then used as a nonlinear discriminating statistic.

Figures 12(a) and (b) show results of the surrogate analysis applied to the screaming data of the juvenile macaque [Fig. 6(a)] and its mother [Fig. 6(b)]. In each figure, local linear prediction errors for the original screaming data and its surrogate data are drawn by varying the embedding dimension $d=3,4,...,15$. Prediction errors of the surrogate data were averaged over 40 sets of different realizations of the surrogate data, where standard deviations are indicated by the error bars. For the local linear prediction, the number of the neighbors was fixed as $\#N=2.4\%$ for the juvenile's analysis and $\#N=2.9\%$ for the mother's analysis. For both juvenile's and mother's screams, it is clear that the original data had much higher SNRs than the surrogate data, where the differences were larger than several standard deviations of the surrogate statistics for all embedding dimensions $d=3,4,...,15$. This implies that the dynamical processes that generated the two macaque screams were not as simple as linear Gaussian. The original screams may have a certain amount of nonlinear dynamics which was well predicted by the nonlinear models. Such nonlinear dynamical structure had been destroyed by the surrogate data shuffling.

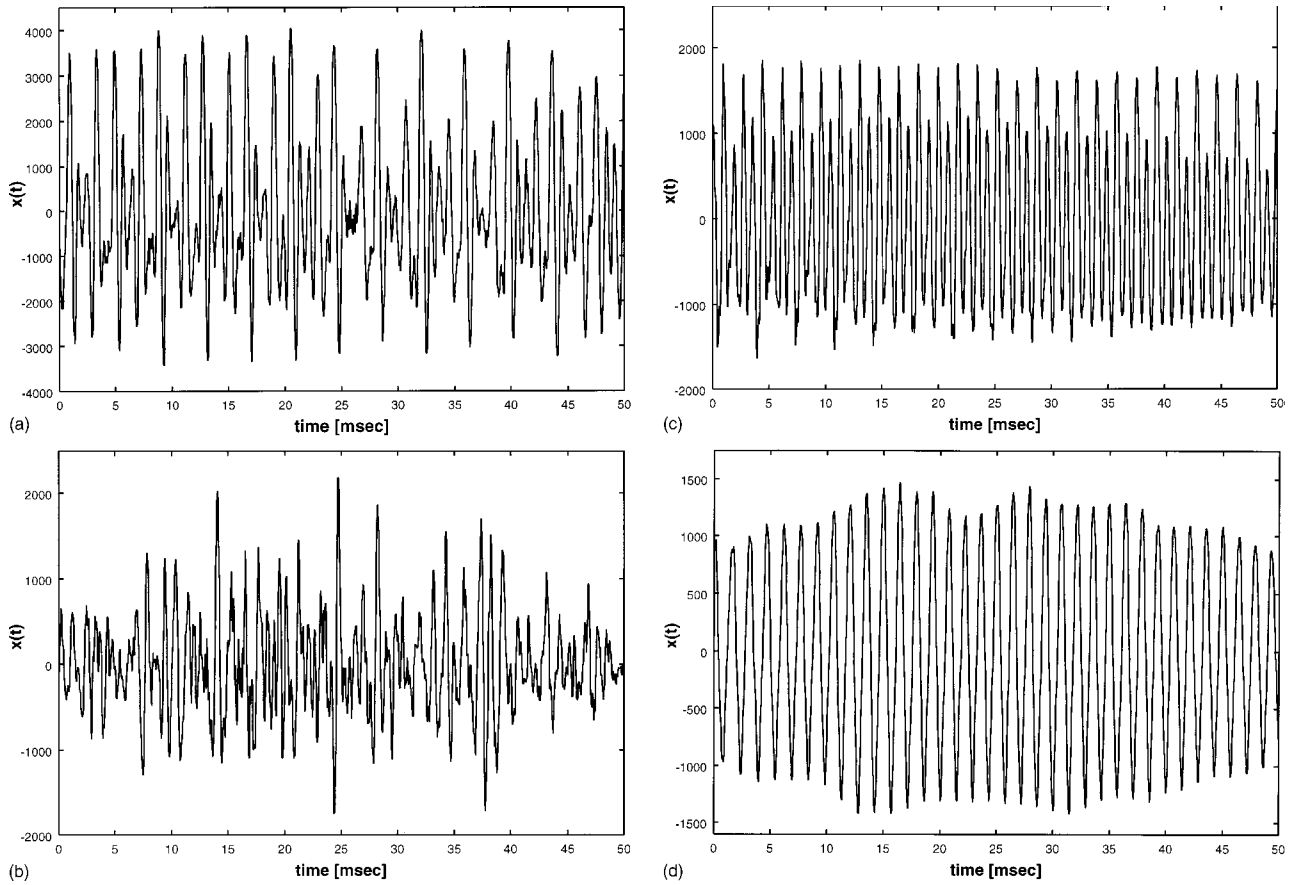

FIG. 10. Waveform structures of various dog barks. (a) and (b) show two different barks from dog a, whereas (c) and (d) show two different barks from dog f.

VII. SUMMARY AND DISCUSSION

Nonlinear analysis was carried out for complex animal vocalizations. As a measure to quantify the amount of nonlinearity in voice data, DVS analysis was applied to three types of animal vocalizations, namely macaque screams, piglet screams, and dog barks. Nonlinear components were detected in all three, particularly for vocalizations with strong harmonics such as limit cycles, subharmonics, and biphonation. In contrast, analysis of highly irregular vocalizations from the three species involved revealed no clear evidence of low-dimensional dynamics. Analyses of 120 dog barks showed good correspondence between the nonlinearity measure LNM and the HNR measure. This result implies that many irregular vocalizations observed in animals can be due to turbulent noise or high-dimensional complex dynamics. However, relatively large nonlinearity measure LNM was computed in some of the irregular vocalizations, such as the juvenile macaque's scream and some of the dog barks. Although careful future investigations are necessary to examine chaos in such real-world data, some of the irregular animal vocalizations seem to be generated from low-dimensional nonlinear dynamics. It is therefore well worth conducting further, detailed investigations of the possible occurrence of chaos in complex animal vocalizations with large nonlinearity measure.

A. Dimensionality of the macaque screams

In the analysis of macaque screams, evidence for low-dimensional nonlinear dynamics was more clearly recognized in the mother's scream than in the juvenile's one. Since the result is obtained from the analysis of only two samples of macaque screams, it is very difficult to judge whether this is a general property of adult and juvenile macaque screams. Nevertheless, it is interesting to consider a relationship between low-dimensional nonlinear dynamics and neural control of animal voice production, because low-dimensionality implies constrained laryngeal dynamics with strong nervous system control. If it is a general property that the dimensionality is lower in the mother's scream than in the juvenile's one, we may say that the mother's call production is more controlled than the juvenile's one. Such a new insight may be useful in understanding normative developmental processes of macaque vocal system. It is therefore a worthy investigation to increase the sample number of the macaque screams used for nonlinear analysis and compare the dimensionality of the adult macaque screams with that of the juvenile macaque screams.

B. Physical interpretation of the dog analysis

In the analysis of dog barks, a wide range of nonlinearity measure LNM was estimated. Let us consider the original causes of these differences. Since all six dogs analyzed by the nonlinear method were from the same breed (dachshund) and expressed similar body sizes, their laryngeal gross anatomy might be similar. We therefore speculate that differences in the acoustic product could come, for instance, from difference in fine (i.e., microscopic) anatomy (e.g., the vocal-

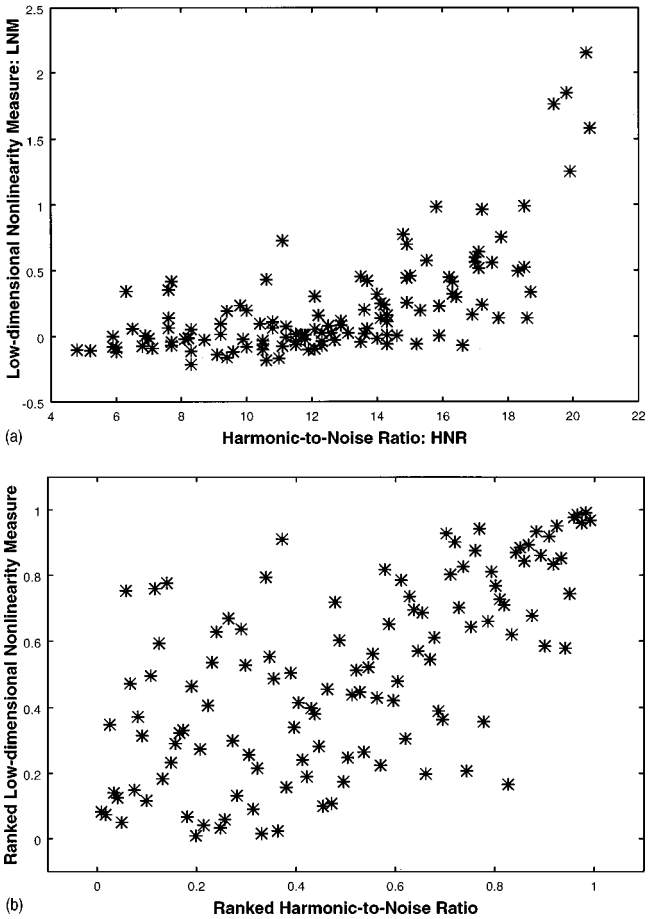

FIG. 11. (a) Correlation plot of the HNR and the nonlinearity measure LNM computed for 120 dog barks. (b) Ranked correlation plot of the HNR and the nonlinearity measure LNM.

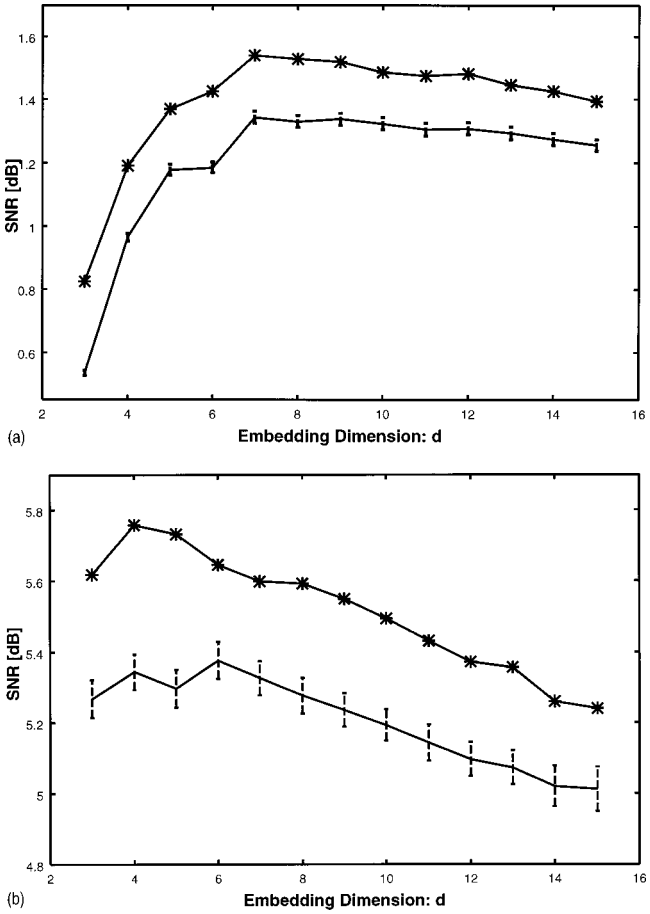

FIG. 12. (a) Nonlinear prediction of the juvenile's scream (solid line with crosses) and its surrogate data (solid line with error bars). (b) Nonlinear prediction of the mother's scream (solid line with crosses) and its surrogate data (solid line with error bars).

fold surface structure) or from differences in the nervous control of the voice production (e.g., vocal-fold parameter and subglottic pressure). In the HNR analysis of the dog barks (Riede *et al.*, 2001), we have earlier discussed that damage to the vocal folds (following hyperphonation) or functional hypertension of the vocal folds could be possible reasons for dog barks that exceeds a normative HNR range. Since the nonlinearity measure LNM was shown to strongly correlate with the HNR, these physical conditions may also give rise to nonlinearity measure that exceeds its normative range.

C. Other applications

In this study, significance of the nonlinear method was tested by using the method of surrogate. There are, however, other approaches to validate nonlinear analysis of animal vocalizations. For instance, there exist ongoing researches on biomechanical modeling of complex animal vocalizations (Mergell *et al.*, 1999; Fee *et al.*, 1998). Such models have been developed to understand the physical and physiological mechanism (e.g., laryngeal oscillations) that generates animal voices. Applying the present nonlinear method to synthetic voice produced from such biomechanical models and comparing the results with those of the real acoustic data might be of significant importance, because (1) such experiment may clarify the sources of nonlinearity which have been (or not have been) detected by the nonlinear method, and (2) plausibility of the biomechanical models can be judged by comparing the nonlinear structure of the model with that of the real acoustic data.

For applications of the present nonlinear analysis technique to other real data, excised larynx (Berry *et al.*, 1996) and EGG data may also provide important materials. Such data can be utilized to examine how the results of nonlinear analysis change as the source of nonlinear phenomena changes. Nonlinear analysis of these types of the measurement data will be carried out in a future work.

D. Usage of the nonlinearity measure

In the analyses of dog barks, there was a strong correlation between the nonlinearity measure LNM and the HNR measure. This is because, for analysis of nonlinear dynamics with strong harmonic components such as limit cycle, subharmonics, and biphonation, the HNR measure works in a similar way as the nonlinearity measure LNM. In the case of analyzing low-dimensional chaos, however, the nonlinearity measure LNM is capable of detecting low-dimensional dynamics, which cannot be detected by the HNR measure. We therefore stress that the nonlinearity measure LNM is useful in particular for analyzing low-dimensional chaos.

Finally, we note that there are limitations in applying the present nonlinear analysis technique to animal vocalizations. Nonstationarity, which is an inherent characteristic of vocalizations, always makes reliable nonlinear analysis quite difficult. Small signal amplitudes, recording noise, and nonlinear distortion in voice signals can also increase nonlinear modeling errors. Very high sampling rate, on the other hand, can sometimes enable linear models to predict nonlinear signals quite accurately, making the difference between nonlinear predictability and linear predictability difficult to interpret. Due to these limitations, some low-dimensional attractors in complex animal vocalizations may remain hidden. For a correct interpretation of complex vocalizations, accompanying simulations of biomechanical models (Mergell *et al.*, 1999; Fee *et al.*, 1998) and conventional spectrographic analysis will certainly be helpful.

[1]In this paper ''noise'' refers to any nonharmonic (irregular) energy within the acoustic utterance signal.

Abarbanel, H. D. I. (**1996**). *Analysis of Observed Chaotic Data* (Springer, New York).

Awan, S. N., and Frenkel, M. L. (**1994**). ''Improvements in estimating the harmonic-to-noise-ratio of the voice,'' J. Voice **8**, 255–262.

Behrman, A. (**1999**). ''Global and local dimensions of vocal dynamics,'' J. Acoust. Soc. Am. **105**, 432–443.

Behrman, A., Agresti, C. J., Blumstein, E., and Lee, N. (**1998**). ''Microphone and electroglottographic data from dysphonic patients: Type 1, 2, and 3 signals,'' J. Voice **12**, 249–260.

Berry, D. A., Herzel, H., Titze, I. R., and Krischer, K. (**1994**). ''Interpretations of biomechanical simulations of normal and chaotic vocal fold oscillations with empirical eigenfunctions,'' J. Acoust. Soc. Am. **95**, 3595–3604.

Berry, D. A., Herzel, H., Titze, I. R., and Story, B. H. (**1996**). ''Bifurcations in excised larynx experiments,'' J. Voice **10**, 129–138.

Bradbury, J. W., and Vehrencamp, S. L. (**1998**). *Principles of Animal Communication* (Sinauer, Sunderland).

Brown, C. H., and Cannito, M. P. (**1995**). ''Modes of vocal variation in Syke's monkey (*Cercopithecus albogularis*) squeals,'' J. Comp. Psych. **109**, 398–415.

Brown, C. H., Alipour, F., Berry, D. A., and Montequin, D. (**2002**). ''Laryngeal biomechanics and vocal communication in the squirrel monkey (*Saimiri boliviensis*),'' J. Acoust. Soc. Am. (submitted).

Casdagli, M. (**1992**). ''Chaos and deterministic versus stochastic nonlinear modeling,'' J. R. Stat. Soc. Ser. B. Methodol. **54**, 303–328.

Davis, P., and Fletcher, N. H., editors (**1996**). *Vocal Fold Physiology: Controlling Complexity and Chaos* (Singular, San Diego).

Farmer, J. D., and Sidorowich, J. J. (**1987**). ''Predicting chaotic time series,'' Phys. Rev. Lett. **59**, 845–848.

Feddersen-Petersen, D. U. (**2000**). ''Vocalization of European wolves (*Canis lupus lupus L.*) and various dog breeds (*Canis lupus f. fam.*),'' Arch. Tierz. Dummerstorf. **43**, 387–397.

Fee, M. S., Shraiman, B., Pesaran, B., and Mitra, P. P. (**1998**). ''The role of nonlinear dynamics of the syrinx in the vocalizations of a songbird,'' Nature (London) **395**, 67–71.

Fischer, J., Hammerschmidt, K., and Todt, D. (**1995**). ''Factors affecting acoustic variation in Barbary macaques (*Macaca sylvanus*) disturbance calls,'' Ethology **101**, 51–66.

Fitch, T., Herzel, H., Neubauer, J., and Hauser, M. (**2002**). ''Calls out of chaos: The adaptive significance of nonlinear phenomena in primate vocal production,'' Anim. Behav. (in press).

Fletcher, N. H. (**2000**). ''A class of chaotic bird calls?'' J. Acoust. Soc. Am. **108**, 821–826.

Gibiat, V., and Castellengo, M. (**2000**). ''Period doubling occurrences in wind instruments musical performance,'' Acust. Acta Acust. **86**, 746–754.

Gouzoules, H., and Gouzoules, S. (**2000**). ''Agonistic screams differ among four species of macaques: The significance of motivation-structural rules,'' Anim. Behav. **59**, 501–512.

Green, S. (**1975**). ''Variation of vocal pattern with social situation in the Japanese monkey (*Macaca fuscata*): A field study,'' in *Primate Behavior* (Academic, New York), pp. 1–102.

Grimm, R. J. (**1967**). ''Catalogue of sounds of the pigtailed macaque (*Macaca nemestrina*),'' J. Zool. Lond. **152**, 361–373.

Hall, K. R. L., and DeVore, I. (**1965**). ''Baboon social behavior,'' in *Primate Behavior: Field Studies of Monkeys and Apes*, edited by I. DeVore (Holt, Rinehart & Winston, New York), pp. 53–110.

Hauser, M. D. (**1993**). ''The evolution of nonhuman primate vocalizations: Effects of phylogeny, body weight, and social context,'' Am. Nat. **142**, 528–542.

Hauser, M. D. (**1996**). *The Evolution of Communication* (MIT Press, Cambridge).

Herzel, H., Berry, D., Titze, I. R., and Saleh, S. (**1994**). ''Analysis of vocal disorders with methods from nonlinear dynamics,'' J. Speech Hear. Res. **37**, 1008–1019.

Hohmann, G. (**1989**). ''Vocal communication of wild bonnet macaques (*Macaca radiata*),'' Primates **30**, 325–345.

Jürgens, U. (**1995**). ''Neuronal control of vocal production,'' in *Current Topics in Primate Vocal Communication*, edited by E. Zimmermann, J. D. Newman, and U. Jürgens (Plenum, New York), pp. 199–206.

Kantz, H., and Schreiber, T. (**1997**). *Nonlinear Time Series Analysis* (Cambridge U.P., Cambridge).

Kubin, G. (**1995**). ''Nonlinear processing of speech,'' in *Speech Coding and Synthesis*, edited by W. B. Kleijin and K. K. Paliwal (Elsevier Science, Amsterdam), pp. 557–610.

Kumar, A., and Mullick, S. K. (**1996**). ''Nonlinear dynamical analysis of speech,'' J. Acoust. Soc. Am. **100**, 615–629.

Lauterborn, W., and Parlitz, U. (**1988**). ''Methods of chaos physics and their application to acoustics,'' J. Acoust. Soc. Am. **84**, 1975–1993.

Markel, J. D., and Gray, A. H. (**1976**). *Linear Prediction of Speech* (Springer, Berlin).

May, R. M. (**1976**). ''Simple mathematical models with very complicated dynamics,'' Nature (London) **261**, 459–467.

Mende, W., Herzel, H., and Wermke, K. (**1990**). ''Bifurcations and chaos in newborn infant cries,'' Phys. Lett. A **145**, 418–424.

Mergell, P., Fitch, T., and Herzel, H. (**1999**). ''Modeling the role of nonhuman vocal membranes in phonation,'' J. Acoust. Soc. Am. **105**, 2020–2028.

Michelsson, K. (**1980**). ''Cry characteristics in sound spectrographic cry analysis,'' in *Infant Communication: Cry and Early Speech*, edited by T. Murry and J. Murry (College-Hill, Houston), pp. 85–105.

Narayanan, S. N., and Alwan, A. A. (**1995**). ''A nonlinear dynamical systems analysis of fricative consonants,'' J. Acoust. Soc. Am. **97**, 2511–2524.

Owren, M. J., and Linker, C. D. (**1995**). ''Some analysis methods that may be useful to acoustic primatologists,'' in *Current Topics in Primate Vocal Communication*, edited by E. Zimmermann, J. D. Newman, and U. Jürgens (Plenum, New York), pp. 1–27.

Paulsen, K. (**1967**). *Das Prinzip der Stimmbildung in der Wirbeltierreihe und beim Menschen* (Akademische, Frankfurt).

Rapp, P. E. (**1993**). ''Chaos in the neurosciences: Cautionary tales from the frontier,'' Biologist **40**, 89–94.

Rapp, P. E., Albano, A. M., Schmah, T. I., and Farwell, L. A. (**1993**). ''Filtered noise can mimic low-dimensional chaotic attractors,'' Phys. Rev. E **47**, 2289–2297.

Riede, T., Wilden, I., and Tembrock, G. (**1997**). ''Subharmonics, biphonations, and frequency jumps: Common components of mammalian vocalization or indicators for disorders,'' Z. Saugetierkunde **62**, Suppl. 2: 198–203.

Riede, T., Herzel, H., Mehwald, D., Seidner, W., Trumler, E., Tembrock, G., and Böhme, G. (**2000**). ''Nonlinear phenomena and their anatomical basis in the natural howling of a female dog–wolf breed,'' J. Acoust. Soc. Am. **108**, 1435–1442.

Riede, T., Herzel, H., Hammerschmidt, K., Brunnberg, L., and Tembrock, G. (**2001**). ''The harmonic-to-noise-ratio applied to dog barks,'' J. Acoust. Soc. Am. **110**, 2191–2197.

Rowell, T. E. (**1967**). ''Agonistic noises of the rhesus monkey (*Macaca mulatta*),'' Symp. Zool. Soc. Lond. **8**, 91–96.

Ruelle, D. (**1990**). ''Deterministic chaos: Science and fiction,'' Proc. R. Soc. London, Ser. A **427**, 244–248.

Ruelle, D. (**1994**). ''Where can one hope to profitably apply the ideas of chaos?'' Phys. Today **7**, 24–30.

Ryan, M. J. (**1988**). ''Constraints and patterns in the evolution of anuran

acoustic communication,'' in *The Evolution of the Amphibian Auditory System*, edited by B. Fritzsch, M. J. Ryan, W. Wilczynski, T. E. Hetherington, and W. Wlakowiak (Wiley, New York), pp. 637–677.
Sauer, T., York, J. A., and Casdagli, M. (**1991**). ''Embedology,'' J. Stat. Phys. **65**, 579–616.
Schassburger, R. M. (**1993**). *Vocal Communication in the Timber Wolf, Canis lupus, Linnaeus* (Paul Parey Sci., Berlin).
Schön, P. C., Puppe, B., Gromyko, T., and Manteuffel, G. (**1999**). ''Common features and individual differences in nurse grunting of domestic pigs (*Sus scrofa*): A multiparametric analysis,'' Behaviour **136**, 49–66.
Schrader, L., and Hammerschmidt, K. (**1997**). ''Computer-aided analysis of acoustic parameters in animal vocalizations: A multiparametric approach,'' Bioacoustics **7**, 247–265.
Schreiber, T., and Schmitz, A. (**1996**). ''Improved surrogate data for nonlinearity tests,'' Phys. Rev. Lett. **77**, 635–638.
Smith, L. A. (**1988**). ''Intrinsic limits of on dimension calculations,'' Phys. Lett. A **133**, 283–288.
Steinecke, I., and Herzel, H. (**1995**). ''Bifurcations in an asymmetric vocal fold model,'' J. Acoust. Soc. Am. **97**, 1571–1578.
Struhsaker, T. T. (**1967**). ''Auditory communication Among vervet monkeys (*Cercopithecus aethiops*),'' in *Social Communication Among Primates*, edited by S. A. Altmann (University of Chicago Press, Chicago), pp. 281–324.
Takens, F. (**1981**). ''Detecting strange attractors in turbulence,'' in *Lecture Notes in Math* (Springer, Berlin, 1981), Vol. 898, pp. 366–381.
Tembrock, G. (**1976**). ''Canid vocalizations,'' Behav. Processes **1**, 57–75.
Tembrock, G. (**1996**). *Akustische Kommunikation bei Saeugetieren* (Wissenschaftl. Buchgesell., Darmstadt).
Theiler, J. (**1986**). ''Spurious dimension from correlation algorithms applied to limited time-series data,'' Phys. Rev. A **34**, 2427–2432.
Theiler, J., Eubank, S., Longtin, A., Galdrikian, B., and Farmer, J. D. (**1992**). ''Testing for nonlinearity in time series: The method of surrogate data,'' Physica D **58**, 77–94.
Theiler, J., and Prichard, D. (**1996**). ''Constrained-realization Monte-Carlo method for hypothesis testing,'' Physica D **94**, 221–235.
Tigges, M., Mergell, P., Herzel, H., Wittenberg, T., and Eysholdt, U. (**1997**). ''Observation and modeling glottal biphonation,'' Acust. Acta Acust. **83**, 707–714.
Titze, I. R. (**1994**). *Principles of Voice Production* (Prentice-Hall, Englewood Cliffs, NJ).
Titze, I. R., Baken, R. J., and Herzel, H. (**1993**). ''Evidence of chaos in vocal fold vibration,'' in *Vocal Fold Physiology*, edited by I. R. Titze (Singular, San Diego), pp. 143–188.
Townshend, B. (**1991**). ''Nonlinear prediction of speech,'' in *Proceedings of the International Conference on Acoustics, Speech, and Signal Processing* (IEEE, New York, 1991), pp. 425–428.
Wilden, I. (**1997**). ''Phonetische variabillitaet in der lautgebung afrikanischer wildhunde (Lycaon pictus) und deren frühe ontogenes,'' Ph.D. thesis, Humboldt-University, Berlin.
Wilden, I., Herzel, H., Peters, G., and Tembrock, G. (**1998**). ''Subharmonics, biphonation, and deterministic chaos in mammal vocalization,'' Bioacoustics, **9**, 171–196.
Yumoto, E., Gould, W. J., and Baer, T. (**1982**). ''Harmonic-to-noise-ratio as an index of the degree of hoarseness,'' J. Acoust. Soc. Am. **71**, 1544–1550.